Available online at www.sciencedirect.com
ScienceDirect
Journal of Crystal Growth 303 (2007) 546–553
JOURNAL OF CRYSTAL GROWTH
www.elsevier.com/locate/jcrysgro

Crystallization conditions of membrane protein CLC-ec1: An example outside the crystallization slot

J. Blouwolff[1], S. Fraden*

Complex Fluids Group, Martin Fisher School of Physics, Brandeis University, Waltham, MA 02454, USA

Received 7 June 2006; received in revised form 6 November 2006; accepted 17 January 2007
Communicated by T.F. Kuech.
Available online 3 February 2007

Abstract

Many soluble proteins crystallize in conditions where their second virial coefficient takes on slightly negative values, known as the crystallization slot, allowing the possibility to screen for crystallizability by measuring virial coefficients. Here we measure virial coefficients for the membrane protein CLC-ec1, which has been crystallized. These virial coefficients reveal that CLC-ec1 crystallization conditions do not correspond to the crystallization slot found for soluble proteins and certain membrane proteins. Additionally, while some membrane proteins crystallize under conditions that are associated with a phase transition of the solubilizing detergent and with attractive detergent interactions, it is demonstrated that this is not the case for CLC-ec1 crystallization. As with many soluble and membrane proteins, CLC-ec1 has been crystallized by adding the neutral polymer poly(ethylene glycol) (PEG). It is shown that the addition of PEG destabilizes detergent micelles and induces CLC-ec1 aggregation in crystallization conditions.

PACS: 87.15.Nn

Keywords: A1. Biocrystallization

1. Introduction

The second virial coefficient of protein solutions, as a probe of protein interactions, has generated a great deal of interest since George and Wilson [1] reported a correlation between protein crystallizability and the second virial coefficient. Their work demonstrated that many water soluble proteins crystallize in conditions where the second virial coefficient becomes slightly negative, indicating net weakly attractive protein interactions. George and Wilson identified values of $-8 \leqslant B_2 \leqslant -0.8 \times 10^{-4}\,\mathrm{mL\,mol\,g^{-2}}$ as the crystallization slot for soluble proteins. For less negative and positive B_2 values, proteins remained in solution, while for more negative B_2 values, precipitation occurred. Is there a similar crystallization slot for membrane protein/detergent complexes (PDCs)? The answer is unclear in part because far fewer membrane proteins have been crystallized than soluble proteins and only a limited number of studies have been performed to quantify membrane protein interactions in crystallization conditions.

Proteins are often crystallized in the presence of additional solutes whose role is to alter the protein phase behavior. Although additives modify the virial description it is still possible to speak of an *effective* protein second virial coefficient which describes protein, or PDC, interactions in solution. Light scattering is a common technique for measuring the virial coefficients of protein solutions and in the case of multicomponent solutions of interest here, one must correctly account for the scattering from each of the components. Simply subtracting the scattering of a solution containing only the additive from the scattering of a mixture of protein and additive is not correct, and in fact doing so yields the *apparent* virial coefficient, which in general is different from the effective

*Corresponding author. Tel.: +1 781 736 2888; fax: +1 781 736 2915.
E-mail addresses: j.blouwolff@gmail.com (J. Blouwolff), fraden@brandeis.edu (S. Fraden).
[1]Present address: Laboratoire de Biologie Chimique ISIS-ULP 8 allée Gaspard Monge, 67083 Strasbourg, France.

0022-0248/$ - see front matter © 2007 Elsevier B.V. All rights reserved.
doi:10.1016/j.jcrysgro.2007.01.028

virial coefficient. The distinction between the apparent and effective virial coefficients is described in detail below. Static light scattering has previously been used to measure the apparent second virial coefficients of PDCs composed of OmpF porin associated with a binary detergent mixture as a function of added poly(ethylene glycol) (PEG) concentration [2]. This work showed that the apparent OmpF PDC second virial coefficient in crystallization conditions falls in roughly the same crystallization slot found for soluble proteins and that the apparent second virial coefficient of OmpF porin PDCs decreases as a function of added PEG concentration. However, this work did not address the distinction between apparent and effective virial coefficients.

In addition to static light scattering, dynamic light scattering, neutron scattering, NMR and chromatographic studies have been carried out to investigate the interactions between PDCs in solution and whether or not attractive PDC interactions and PDC aggregation are observed prior to crystallization. Neutron scattering studies on the reaction centers from *Rhodobacter sphaeroides* R-26 associated with the detergents lauryl-dimethylamine-N-oxide (LDAO) or *n*-octyl-β-glucoside (OG) [3] found that although the addition of PEG to a PDC solution induces crystallization, it does not lead to aggregation prior to crystallization. Tanaka et al. [4] performed dynamic light scattering studies of cytochrome bc_1 complex associated with sucrose monolaurate and found evidence that the addition of PEG induces attraction between bc_1 PDCs in crystallization conditions.

Detergents are needed to solubilize membrane proteins in aqueous solvents due to the hydrophobic nature of the proteins' transmembrane domains. Therefore, it is reasonable to suppose that PDC interactions reflect the interactions between PDC detergent moieties. Noting this, Rosenbusch [5] suggested that PDC crystallization should be favored in conditions where detergent micellar interactions are attractive. Studies of OmpF porin [2,6] show that its crystallization occurs in conditions where the detergent micelle interactions are attractive and where the detergent, in the absence of the protein, undergoes a phase transition. Hitscherich [2], among others, hypothesize that the observed correlation between detergent cloud point and PDC crystallization is explained if both phenomena arise from attractions of similar magnitude between detergent molecules. Recently, Berger et al. [7] used self-interaction chromatography and cloud point studies to demonstrate that bacteriorhodopsin/OG PDC interactions become more attractive as the detergent phase transition is approached and more generally that detergent micellar interactions and structure significantly influence PDC interactions.

In this work virial coefficients are measured for PDCs composed of the membrane protein, CLC-ec1, and the non-ionic detergent, *n*-octyl-β-maltoside (OM) to determine if CLC-ec1 falls in the crystallization slot, if the crystallizing precipitant PEG induces attractions and aggregation, and to determine the difference between the apparent and effective virial coefficients. We also investigate whether or not a detergent phase transition is associated with the crystallization of CLC-ec1 PDCs.

2. Theory

We treat PDC/PEG solutions as two component mixtures. Virial coefficients in a two component mixture are defined by expanding the mixture's excess Gibbs free energy relative to that of the solvent (G) in powers of the densities of the two independent solutes, labeled 1 and 2.

$$\frac{G}{Vk_BT} = \rho_1 \ln \rho_1 + \rho_2 \ln \rho_2 + B_{11}\rho_1^2 + 2B_{12}\rho_1\rho_2 + B_{22}\rho_2^2 + C_{111}\rho_1^3 + 3C_{112}\rho_1^2\rho_2 + \cdots. \quad (1)$$

In Eq. (1) $\rho_i = N_i/V$ (Vol^{-1}); k_B is Boltzmann's constant; T is the absolute temperature; B_{ij} [Vol] are the second virial coefficients and C_{ijk} [Vol^2] are the third virial coefficients. With this notation the second virial coefficient often denoted by B_2 is written as B_{ii}. Virial coefficients are related to integrals of the interaction potential energy between molecules [8]. The subscript 1 shall refer to the PDCs and the subscript 2 to the PEG. In what follows it is assumed that the term containing ρ_1^3 is negligible since the PDC concentration is dilute. It was found experimentally that the term containing ρ_2^3 was negligible from light scattering of PEG alone in solution. The conversion of virial coefficients from volume units to experimentally convenient light scattering units is given by $B_{ij}\ (\mathrm{mL\,mol\,g^{-1}}) = B_{ij}\ (\mathrm{mL})N_A/(M_iM_j)$ and $C_{ijk}\ (\mathrm{mL^2\,mol\,g^{-3}}) = C_{ijk}\ (\mathrm{mL^3})N_A^2/(M_iM_jM_k)$ where M_i ($\mathrm{g\,mol^{-1}}$) are the solute molecular weights and N_A ($\#\,\mathrm{mol^{-1}}$) is Avogadro's number.

Virial coefficients are measured by static light scattering experiments. Previous analyses of light scattering from two solute protein systems [2,9] have employed an effective one solute framework. Such an analysis ignores interference in the scattered light from different components and can lead to incorrect virial coefficient values. Therefore, the light scattering data from detergent/PEG and PDC/PEG mixtures is analyzed using the multicomponent analysis developed by Kirkwood and Goldberg [10] and others [11], which has been previously applied to soluble protein/polymer mixtures [12,13]. The excess light scattering of a two solute system (R_{1+2}) over that of a single solute system (R_2) can be written as [10]

$$\frac{Kc_1}{R_{1+2} - R_2} = \alpha + \beta \times c_1. \quad (2)$$

Here $K = 2(\pi n_o n_1)^2/N_A\lambda^4$ where n_o is the solvent refractive index, $n_i = \partial n/\partial c_i$ is the refractive index increment of solute i, N_A is Avogadro's number, λ is the wavelength of the incident radiation in vacuum, c is the solute weight concentration and R is the Rayleigh ratio. Eq. (2) has the same form as the one component scattering equation $Kc/R = 1/M_1 + 2B_{11c}$ where M_1 is the solute molecular weight. In Eq. (2) α is the inverse of the apparent molecular

weight and $\beta/2$ is the apparent second virial coefficient. In a multicomponent solution α and β depend on the added polymer properties (M_2, n_2), concentration c_2, and the protein/polymer interaction (B_{12} and C_{112}) [10]:

$$\alpha = 1/M_1 + 4c_2 m B_{12}, \tag{3}$$

where $m = M_2 n_2 / M_1 n_1$. B_{12} may be calculated from measurements of α as a function of polymer concentration c_2. β is given by

$$\beta = 2[B_{11}^{\text{eff}} + mc_2(3C_{112} + 2B_{11}B_{12}M_1)], \tag{4}$$

with $B_{11}^{\text{eff}} = B_{11} + c_2[(3C_{112} - 2B_{12}^2 M_2)]$. C_{112} is obtained from measurements of β as a function of c_2 since all the other quantities in Eq. (4) are determined independently. It is possible to view a two component PDC/PEG solution as an effective one component PDC solution where the PDC interactions are modified by the addition of PEG. In principle, the protein's molecular weight and effective PDC second virial coefficient, B_{11}^{eff}, can be obtained experimentally by the addition of invisible polymers ($n_2 = m = 0$) to the PDC solution [14,15]. However, we do not index match the polymer ($n_2 \neq 0$). Instead we measure the virial coefficients and calculate B_{11}^{eff}. B_{11}^{eff} represents the *effective* interactions felt between PDCs in solution in the presence of PEG, whereas β represents the *apparent* second virial coefficient obtained from light scattering experiments. As we have shown, α and β depend on optical parameters and thus do not correctly reflect the molecular weight or effective protein–protein interaction.

If PEG interacts only sterically with PDCs, then PEG induces attraction between PDCs due to the depletion effect and $\partial B_{11}^{\text{eff}}/\partial c_2 < 0$ [16]. In contrast to the depletion effect, if $\partial B_{11}^{\text{eff}}/\partial c_2 > 0$ then the addition of polymer induces PDC repulsion [13].

In addition to the PDC and PEG there are also free OM micelles; therefore treating the PDC/PEG solution as a two component mixture is a simplification. The PDC complex has a molecular weight approximately seven times that of a free OM micelle. It will turn out that the concentration of PDC and free OM micelles are similar in our experiments and since the intensity of scattered light scales with the square of the mass of the scattering object the total intensity scattered from free OM micelles will be 50 times smaller than the scattered intensity from the PDCs, which justifies neglecting the scattering contribution from the OM micelles.

3. Materials and Methods

The putative Cl^- channel protein, CLC-ec1, was first expressed and purified by Maduke et al. [17]. CLC-ec1 was crystallized in two dimensions by Mindell et al. [18] who obtained a 6.5 Å resolution projection structure of CLC-ec1. Single channel electrophysiological recordings of CLC-ec1 have been obtained by Accardi et al. [19] who subsequently showed that CLC-ec1 functions as a H^+–Cl^- exchange transporter [20]. CLC-ec1 was crystallized in three dimensions and its structure solved to 3.0 Å from X-ray scattering experiments by Dutzler et al. [21]. The CLC-ec1 crystal packing shows that crystal contacts between neighboring CLC-ec1 molecules in the crystal are made between the polar residues. In this work CLC-ec1 was expressed and purified as described by Dutzler et al. [21].

DM (sol-grade) and OM (anagrade) were obtained from Anatrace. PEG of nominal molecular weight 400 g mol^{-1}, designated as PEG400, was obtained from Sigma. The OM and PEG were dissolved in the published CLC-ec1 crystallization buffer [21] which consists of a (1:1) mixture of (75 mM NaCl and 10 mM Tris-HCl at pH 7.5 : 50 mM Na_2SO_4, 50 mM Li_2SO_4 and Tris 50 mM at pH 8.5). The CLC-ec1 concentrations were measured by UV absorption at a wavelength of 280 nm using an extinction coefficient $\varepsilon_{280\text{nm}} = 0.85\,\text{mL mg}^{-1}\,\text{cm}^{-1}$ calculated from the CLC-ec1 sequence [17]. The precise value of the extinction coefficient does not effect the value of β, since β is a ratio of concentrations.

In order to verify that our light scattering experiments were performed in CLC-ec1 crystallization conditions [21], crystals of CLC-ec1 were grown in sitting drops at $T = 20\,^{\circ}\text{C}$ by equilibrating a (1:1) mixture of protein and reservoir solution against the reservoir. We label the time when the protein and reservoir solutions were mixed and the start of crystallization trials as $t = 0$. The protein solution consisted of 20 mg mL^{-1} CLC-ec1 in 45 mM OM, 75 mM NaCl and 10 mM Tris-HCl at pH 7.5. The reservoir solution consisted of 330 mg mL^{-1} PEG400 in 50 mM Na_2SO_4, 50 mM Li_2SO_4 and Tris 50 mM at pH 8.5. Crystals were observed after one week as shown in Fig. 1. These crystals were assumed to be made of CLC-ec1 because sitting drops without added CLC-ec1 showed

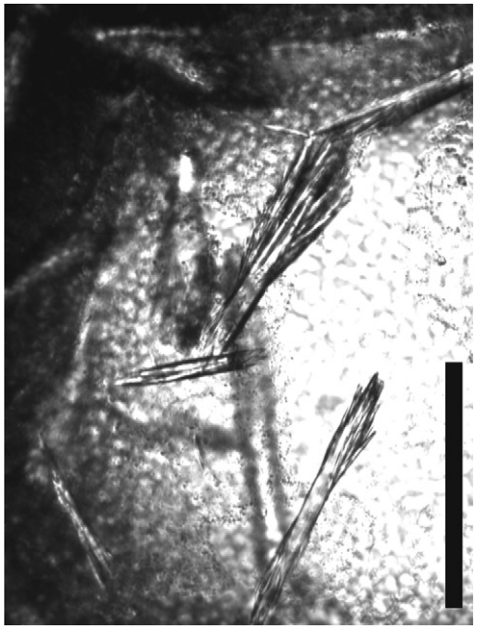

Fig. 1. A bright field optical micrograph of CLC-ec1 crystals is shown. Crystals were found using reservoir PEG concentrations of 320 and 330 mg mL^{-1}. The scale bar indicates 100 μm.

no crystals, nor did sitting drops with CLC-ec1, but without added PEG in the reservoir.

Refractive index increments were measured using a Brookhaven Instruments differential refractometer at $\lambda = 620\,\text{nm}$. For PEG400 in the CLC-ec1 crystallization buffer $\partial n/\partial c_{\text{PEG400}} = 1.33 \times 10^{-4}\,\text{mL mg}^{-1}$ independent of T for $10\,^{\circ}\text{C} \leqslant T \leqslant 40\,^{\circ}\text{C}$; for OM in the CLC-ec1 crystallization buffer at $T = 20\,^{\circ}\text{C}$, $\partial n/\partial c_{\text{OM}} = 1.07 \times 10^{-4}\,\text{mL mg}^{-1}$. For CLC-ec1/OM PDCs $\partial n/\partial c$ was not measured in order not to waste precious PDC sample. Instead, we set $\partial n/\partial c_{\text{PDC}} = 2 \times 10^{-4}\,\text{mL mg}^{-1}$. This value of $\partial n/\partial c$ is a rough estimate based on the value of $\partial n/\partial c$ for soluble proteins such as lysozyme ($\partial n/\partial c_{\text{lys}} = 1.85 \times 10^{-4}$) and BSA ($\partial n/\partial c_{\text{BSA}} = 1.85 \times 10^{-4}$). Using $\partial n/\partial c_{\text{PDC}} = 2 \times 10^{-4}\,\text{mL mg}^{-1}$ yields a PDC molecular weight of $M_1 = 1/\alpha = 1.11 \pm 0.04 \times 10^5\,\text{g mol}^{-1}$and an apparent second virial coefficient of $\beta/2 = 3 \times 10^{-4}\,\text{mL mol/g}^2$ in the CLC-ec1 crystallization buffer at $T = 20\,^{\circ}\text{C}$. This value of the PDC molecular weight is consistent with a CLC-ec1 dimer [17] with approximately 20 associated OM molecules.

The static and dynamic light scattering experiments (SLS and DLS) were performed using an ALV goniometer and correlator system. All of our light scattering experiments were performed in the *vu* polarization mode. Absolute Rayleigh ratios of aqueous solutions for SLS were determined by using pure toluene as a standard whose Rayleigh ratio is $1.35 \times 10^{-5}\,\text{cm}^{-1}$ at 633 nm and $T = 20\,^{\circ}\text{C}$. [22]. DLS measures the intensity autocorrelation function $f_1(t) = \langle I(t_o)I(t_o + t)\rangle$ where $I(t)$ is the scattered intensity as a function of time at a given scattering angle. For a single diffusing solute species the intensity autocorrelation function decays exponentially $f_1(t) = a\mathrm{e}^{-\Gamma t}$. The diffusion constant (D) is calculated from $D = \Gamma/q^2$ where q is the amplitude of the scattering vector. All SLS and DLS experiments were performed at a scattering angle of $\theta = 90^{\circ}$ for which $q = 1.87 \times 10^7\,\text{m}^{-1}$. When multiple diffusing species contribute to the time variation of the scattered intensity, the autocorrelation function becomes an integral of exponentials:

$$f_1(t) = \int \mathrm{e}^{-\Gamma t} F_{\text{i}}(\Gamma)\,\mathrm{d}\Gamma, \tag{5}$$

where $F_{\text{i}}(\Gamma)$ is the intensity weighted decay rate distribution function. The cumulant method is also used to analyze $f_1(t)$ [23]: $\ln(f_1(t)) = \ln a - \bar{\Gamma}t + (\mu_2/2)t^2 - (\mu_3/6)t^3 + \cdots$. Then the apparent diffusion constant is $\bar{D} = \bar{\Gamma}/q^2$. Hydrodynamic radii r_{H} were obtained from DLS measurements via the Stokes–Einstein relation [24]: $r_{\text{H}} = k_B T/(6\pi\eta\bar{D})$ where η is the solvent viscosity. The intensity weighted distribution function may also be expressed in terms of the apparent hydrodynamic radii, rather than decay rates, to find $F_{\text{i}}(r)$. The distribution functions shown in Fig. 6 were calculated using the ALV-NonLin software which implements the CONTIN algorithm to calculate $F_{\text{i}}(r)$ via an inverse Laplace transform of $f_1(t)$. We treat the aggregating proteins as a distribution of spheres of mass $M(r) = \rho 4\pi r^3/3$ and density ρ and assume that the intensity of scattered light is of the form $F_{\text{i}}(r) \propto M^2(r)F_{\text{N}}(r)P(qr)$ with $F_{\text{N}}(r)$ the number of particles of radius r and the form factor of a sphere $P(qr) = 3(\sin(qr) - qr\cos(qr)/(qr)^3)^2$. The mass weighted distribution function, $F_{\text{m}}(r) = M(r)F_{\text{N}}(r)$, is calculated from the intensity weighted distribution function as $F_{\text{m}}(r) \propto F_{\text{i}}(r)/(M(r)P(qr))$.

4. Results

We first present results from light scattering experiments on PEG solutions, OM solutions and OM/PEG mixtures in the CLC-ec1 crystallization buffer. SLS experiments on PEG400 show $M_2 = 400 \pm 100\,\text{g mol}^{-1}$, $B_{22}(T = 20\,^{\circ}\text{C}) = 0.013\,\text{mL mol g}^{-2}$ and $\partial B_{22}/\partial T = -1.6 \times 10^{-4}\,\text{mL mol g}^{-2}\,^{\circ}\text{C}^{-1}$. From dynamic light scattering experiments we measured $r_{\text{H}} = 0.7\,\text{nm}$ for PEG400 in the dilute limit. At PEG400 concentrations greater than $160\,\text{mg mL}^{-1}$ a second, slower decaying mode appears in the DLS correlation function data.

The critical micellar concentration (cmc) of OM was determined by measuring the scattered intensity as a function of OM concentration [2] and making a linear fit to the concentration dependence of the scattering. The cmc was identified as the OM concentration where the scattered intensity extrapolated to zero, as shown in panel (a) of Fig. 2. The hydrodynamic radius (r_{H}) measured by DLS in the same OM samples was monitored simultaneously. The hydrodynamic radius drops sharply with decreasing OM concentration at the cmc, as shown in panel (b) of Fig. 2. The cmc of OM in water is $9\,\text{mg mL}^{-1}$ [25]. For OM in the ClC-ec1 crystallization buffer at $T = 20\,^{\circ}\text{C}$ the cmc as a function of added PEG400 concentration is shown in panel (a) of Fig. 3. The concentration of OM micelles was calculated as the bulk OM concentration minus the cmc. From the cmc data, the free energy difference between a

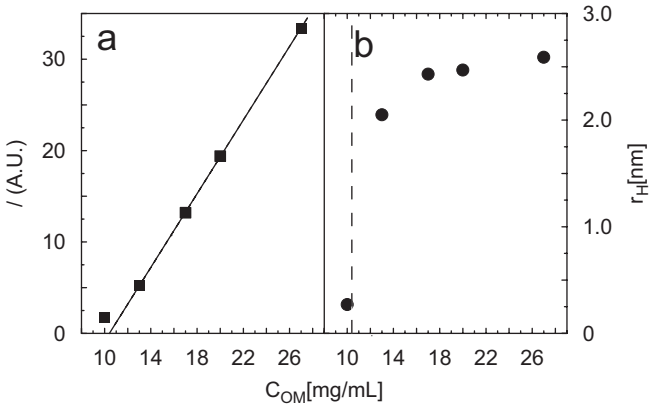

Fig. 2. Panel (a) The time average of the scattered light intensity I versus concentration of *n*-octyl-β-maltoside (OM) dissolved in the CLC-ec1 crystallization buffer with no added PEG at $T = 20\,^{\circ}\text{C}$. The cmc was identified from a linear fit to the scattered intensity I, in arbitrary units, as a function of OM concentration as the extrapolated point where $I = 0$. Panel (b) displays the hydrodynamic radius (r_{H}) measured by dynamic light scattering in the same samples. The dashed line in panel (b) shows the location of the CMC found from panel (a).

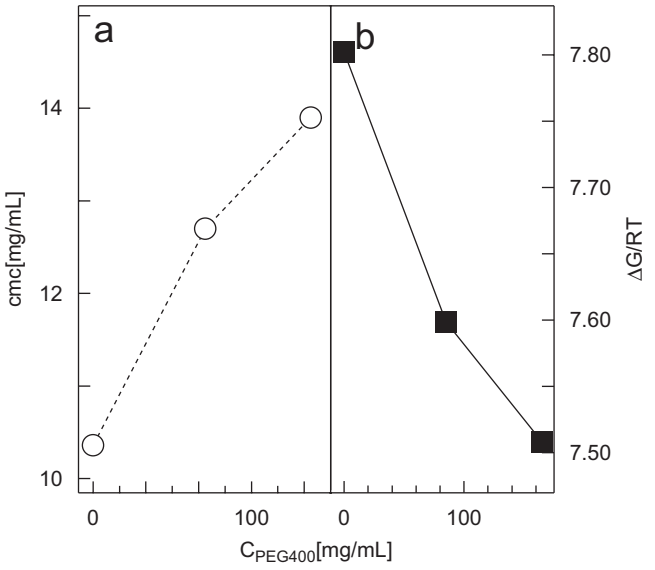

Fig. 3. The critical micellar concentration (cmc) of *n*-octyl-β-maltoside (OM) is shown in panel (a) as a function of added PEG400 concentration in the CLC-ec1 crystallization buffer at $T = 25\,^{\circ}\mathrm{C}$. Panel (b) displays the dimensionless free energy difference ($\Delta G/RT$) between an OM molecule in the bulk and in a micelle calculated via Eq. (6) as a function of PEG400 concentration.

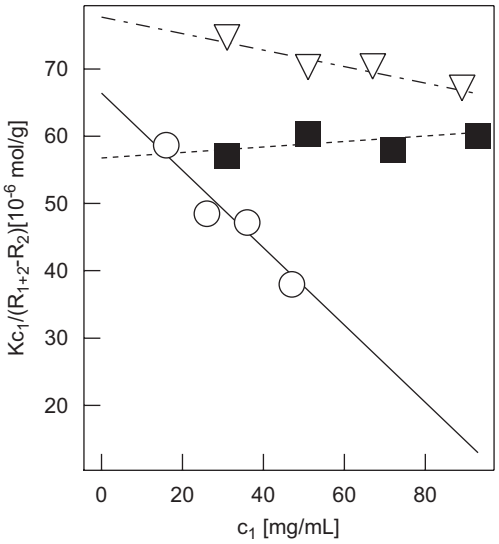

Fig. 4. Light scattering from OM micelles and OM/PEG400 mixtures is shown where the micelles are labeled with the subscript 1 and the PEG is labeled with the subscript 2. The scattering ratio from Eq. (2), $Kc_1/(R_{1+2} - R_2)$, is plotted as a function of OM micellar concentration, c_1 for no added PEG400 (○), for PEG400 85 mg mL^{-1} (■) and for PEG400 165 mg mL^{-1} (▽). The lines are linear fits to Eq. (2) from which α and β listed in Table 2 are extracted.

detergent molecule free in the bulk and in a micelle (ΔG) is calculated by

$$\frac{\Delta G}{RT} = -\ln X_{\mathrm{cmc}}, \tag{6}$$

where R is the gas constant, T is the absolute temperature and X_{cmc} is the cmc expressed as a mole fraction. As shown in Fig. 3 panel (a) the cmc of OM increases as a function of increasing PEG400 concentration, whereas panel (b) shows that the free energy difference between a detergent molecule in the bulk and in a micelle decreases as PEG400 is added. These data indicate that the addition of PEG makes micelle formation less favorable and in effect destabilizes micelles with respect to free detergent monomers.

OM shows no phase transition as a function of temperature up to concentrations of greater than 500 mg mL^{-1} when dissolved in pure water [25]. All detergent concentrations in this study were less than 50 mg mL^{-1}, but detergent phase behavior depends sensitively on the buffer conditions. Therefore, in order to determine whether or not an OM phase transition occurs in the CLC-ec1 crystallization buffer, samples of OM at concentrations up to 50 mg mL^{-1} in the CLC-ec1 crystallization buffer with added PEG400 165 mg mL^{-1} were observed by bright field microscopy in the temperature range $2 \leqslant T \leqslant 95\,^{\circ}\mathrm{C}$. No clouding transitions were observed indicating that no detergent phase transition is associated with the crystallization conditions of CLC-ec1.

Static light scattering experiments were performed on OM micelles with and without PEG400 in order to determine the detergent interactions in CLC-ec1 crystallization conditions. Data from SLS experiments on OM micelles at $T = 25\,^{\circ}\mathrm{C}$ in the CLC-ec1 crystallization buffer are shown in Fig. 4. Without PEG these data yield a micellar molecular weight of $14\,286 \pm 1500$ g mol^{-1}, or a micellar aggregation number of approximately $N_{\mathrm{OM}} = 31$. At this same temperature $\beta = -6 \pm 1 \times 10^{-4}$ mL mol g^{-2} and $\partial\beta/\partial T = 1.7 \pm 0.5 \times 10^{-5}$ mL mol g^{-2} $^{\circ}$C^{-1}. In these conditions the OM micellar interactions are therefore attractive. For OM/PEG400 mixtures the subscript 1 refers to OM micelles and the subscript 2 to PEG400. α and β from the data in Fig. 4 are shown in Table 2 and were fit to Eqs. (3,4) from which $B_{12} = 1.5 \pm 0.7 \times 10^{-4}$ mL mol g^{-2} and $C_{112} = 5 \pm 1.4 \times 10^{-4}$ mL^2 mol g^{-3} were obtained, assuming that the micellar molecular weight does not change as a function of added PEG. This assumption cannot be verified with these data. The α and β data are not fit well by the multicomponent light scattering model of Eqs. (3, 4) indicating that the addition of PEG may change the micellar aggregation number and micellar structure. However, this model does place constraints on the effect of PEG on OM micellar interactions. Since β increases with increasing PEG concentration, PEG does not induce more attraction between OM micelles. Quantitatively, the fitted values of B_{12} and C_{112} lead to $\partial B_{11}^{\mathrm{eff}}/\partial c_2 \geqslant 0$. If we assume that the micellar molecular weight remains constant as PEG400 is added, then we conclude that adding PEG400 to OM micelles decreases the attractions between OM micelles, which is opposite to the prediction of polymer induced depletion attraction.

In order to determine whether or not the crystallization of CLC-ec1 occurs in the crystallization slot, the light scattering parameters α and β were measured for CLC-ec1 PDCs as shown in Fig. 5. The values of α and β for CLC-ec1/OM PDCs are given in Table 1 with and without added PEG400 showing that $\beta>0$ and that β is essentially unchanged as PEG is added. In these measurements PEG400 was added to the PDC solution at $t=0$. All static light scattering data was taken between $0<t<0.5$ h. Since $\beta>0$ without PEG, the PDC interactions as measured by the apparent virial coefficient are repulsive, which is expected in non-crystallizing conditions. β of just OM micelles in solution increases significantly as PEG is added in this PEG400 concentration range, while β of the PDCs remains constant as PEG is added. Therefore, the apparent PDC virial coefficient, β, does not track the evolution of β for the OM micelles. For CLC-ec1/OM PDCs $\beta>0$ in the crystallization conditions indicating that the crystallization of these PDCs occurs outside the crystallization slot found for soluble proteins and other membrane proteins [see also Table 2].

Since β for CLC-ec1 PDCs remains constant, or slightly decreases as PEG is added, it would appear that PEG induces weak PDC attractions. However, β is the apparent virial coefficient and does not represent the PDC interactions. Therefore, it is necessary to calculate the variation of the effective PDC virial coefficient with PEG concentration $\partial B_{11}^{\mathrm{eff}}/\partial c_2$ in order to conclude whether PEG induces PDC attraction or repulsion. In order to calculate $\partial B_{11}^{\mathrm{eff}}/\partial c_2$ one must find the mixed virial coefficients B_{12} and C_{112}. From the values of α and β in Table 1 the mixed virial coefficient values are found from Eqs. (3) and (4): $B_{12}=-4.2\pm1.2\times10^{-3}\,\mathrm{mL\,mol\,g^{-2}}$ and $C_{112}=4.8\pm1.7\times10^{-3}\,\mathrm{mL^2\,mol\,g^{-3}}$. For any net repulsive polymer/PDC interaction $B_{12}>0$. The measured value of $B_{12}<0$ indicates that the PDCs have a net attraction to PEG molecules. The values of B_{12} and C_{112} allow us to calculate the variation of the effective virial coefficient for CLC-ec1/OM complexes as a function of PEG concentration: $\partial B_{11}^{\mathrm{eff}}/\partial c_2=2.9\pm1.3\times10^{-4}\,\mathrm{mL^2\,mol\,g^{-3}}$. Since $\partial B_{11}^{\mathrm{eff}}/\partial c_2>0$ the PDC interactions are becoming more repulsive as PEG is added, contrary to the conclusion reached from considering only the apparent virial coefficient, β where one would obtain $\partial\beta/\partial c_2=-6.4\pm1.6\times10^{-4}\,\mathrm{mL^2\,mol\,g^{-3}}<0$. The fact that $\partial B_{11}^{\mathrm{eff}}/\partial c_2>0$, whereas $\partial\beta/\partial c_2<0$ leads to qualitatively different conclusions concerning the effect of PEG on protein interactions demonstrates the importance of using a multicomponent approach to analyze light scattering of protein mixtures [13].

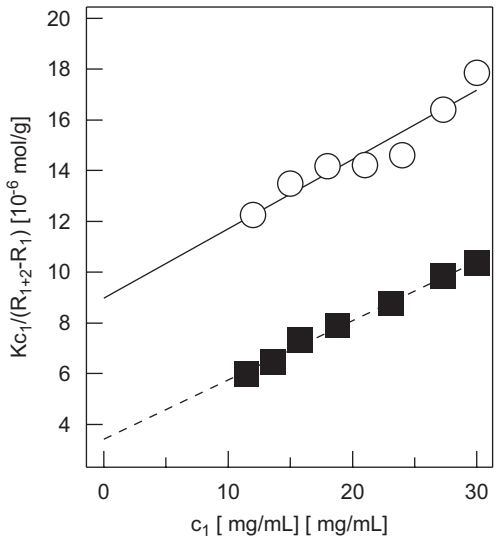

Fig. 5. Light scattering from PDCs and PDC/PEG400 mixtures is shown. Here the subscript 1 refers to the PDCs and the subscript 2 refers to PEG400. The scattering ratio from Eq. (2), $Kc_1/(R_{1+2}-R_2)$, is plotted as a function of CLC-ec1 concentration, c_1 for no added PEG400 (○) and for PEG400 165 mg mL^{-1} (■). The lines are linear fits to Eq. (2) from which α and β listed in Table 1 are extracted.

In order to assess whether or not PDC aggregation occurs in crystallizing conditions, DLS experiments were performed simultaneously with the virial coefficient measurements. The DLS results show that PEG induces PDC aggregation on the time scale of hours, whereas crystallization occurs on the time scale of a number of days. The intensity weighted distribution function of hydrodynamic radii ($F_i(r)$) of PDC/PEG mixture is shown in Fig. 6. The distribution function at the start of crystallization trials approximately 12 h after the final purification step, just before the PEG is added, mainly consists of a large peak indicating single PDCs existing in solution and a small amount of aggregates. In the presence of PEG at $t=0$, as shown in panel (b) of Fig. 6, the distribution function differs from that without added PEG due to a slow mode associated with the relatively high PEG400 concentration of 165 mg mL^{-1}. In panel (b) of Fig. 6, an aggregate peak appears and grows with time as the first peak shrinks indicating that PDCs aggregate in the presence of PEG400, whereas panel (a) of Fig. 6 shows that without PEG the small fraction of PDC aggregates remains essentially

Table 1
Apparent and effective virial coefficients of PDC/PEG mixtures

c_{PEG400} (mg mL^{-1})	α (10^{-6} mol g^{-1})	β (10^{-4} mL mol g^{-2})	B_{11}^{eff} (10^{-4} mL mol g^{-2})
0	9 ± 1	3 ± 0.5	3 ± 0.5
165	3 ± 1	2 ± 0.5	3.5 ± 0.6

α, the inverse of the apparent molecular weight, and β, twice the apparent second virial coefficient, determined by light scattering for CLC-ec1/OM, protein/detergent complexes at $T=25\,^{\circ}$C are shown without any added PEG400 and in the presence of PEG400 165 mg mL^{-1} used in the CLC-ec1 crystallization conditions. The PDC effective second virial coefficient B_{11}^{eff} calculated from α and β is also listed.

Table 2
Apparent virial coefficients of *n*-octyl-*β*-maltoside (OM)

c_{PEG400} (mg mL^{-1})	α (10^{-5} mol g^{-1})	β (10^{-4} mL mol g^{-2})
0	7 ± 0.6	-5.5 ± 0.4
85	6 ± 0.4	0.2 ± 0.3
165	8 ± 0.5	-0.7 ± 0.5

α, the inverse of the apparent molecular weight, and β, twice the apparent second virial coefficient, determined from Fig. 4 for OM micelles at $T = 25\,^{\circ}$C are shown without and with added PEG400 in the CLC-ec1 crystallization conditions. From these data $B_{12} = 1.5 \pm 0.7 \times 10^{-4}$ mL mol g^{-2} and $C_{112} = 5 \pm 1.4 \times 10^{-4}$ mL^2 mol g^{-3} were determined via Eqs. (3), (4).

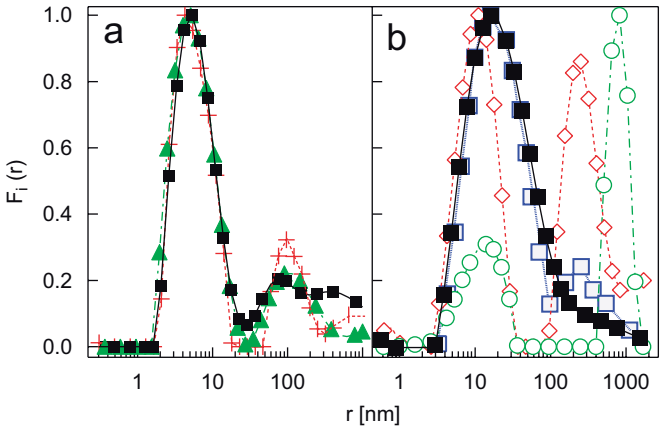

Fig. 6. The PDC intensity weighted distribution function of hydrodynamic radii ($F_i(r)$) obtained by dynamic light scattering, Eq. (5), for CLC-ec1/OM in the crystallization buffer at $T = 20\,^{\circ}$C is shown in panel (a), without added PEG, and in panel (b) with PEG400 165 mg mL^{-1}, at different times. The addition of PEG marks the beginning of the crystallization trial ($t = 0$) and occurred 12 h after the final purification step. Panel (a) shows insignificant aggregation occurs from $t = 0$ (■) to $t = 15$ min (+) to $t = 14$ h (▲). Panel (b) shows that adding PEG to a dispersion of CLC-ec1/OM PDCs induced PDC aggregation. In panel (b) the decay time distribution is shown at $t = 0$ (■), $t = 0.5$ h (□), $t = 2$ h (◇) and $t = 4$ h (○). As time progresses, the peak corresponding to large aggregates grows and the peak corresponding to individual PDCs shrinks indicating PDC aggregation.

constant as a function of time. The distributions shown in Fig. 6 are weighted by the intensity of the scattered light and are therefore sensitive to large aggregates. Calculation of the mass weighted distribution function of the data shown in Fig. 6 reveals that the fraction of the total PDC mass in the aggregate peak increases to $50 \pm 3\%$ at $t = 4$ h, although the number of PDC aggregates remains less than $1 \pm 0.5\%$ of the number of non-aggregated PDCs at $t = 4$ h. Therefore, PEG induces the formation of a few, large PDC aggregates. If the PEG is removed from the PDCs after a period of aggregation, DLS shows that the aggregates remain intact (data not shown) indicating that PEG induced PDC aggregation is irreversible.

It must be considered whether or not PDC aggregation in the presence of PEG can change the conclusion that PEG does not induce PDC attraction on the virial coefficient level, i.e. $\partial B_{11}^{\mathrm{eff}}/\partial c_2 > 0$. The analysis of the virial coefficients presented above was based on the assumption that the PDC molecular weight remained constant, which is clearly not the case in light of the PDC aggregation. The PDC aggregation shown in Fig. 6 means that the two component analysis of light scattering data presented above is not strictly applicable. However, the static light scattering data was measured between $0 < t < 0.5$ h. At $t = 0.5$ h the DLS data as shown in panel (b) of Fig. 6 are consistent with an approximately 30% increase in the PDC molecular weight. If we assume such an increase in the PDC molecular weight along with the data in Table 1, we can use Eqs. (3), (4) to recalculate $\partial B_{11}^{\mathrm{eff}}/\partial c_2$. A 30% change in the PDC molecular weight leads to $\partial B_{11}^{\mathrm{eff}}/\partial c_2 = 2.8 \pm 0.8 \times 10^{-3}$ mL^2 mol g^{-3}. Alternatively, if we ask what increase in PDC molecular weight would be necessary to yield $\partial B_{11}^{\mathrm{eff}}/\partial c_2 = 0$, or equivalently, to change the effective interaction from repulsive to attractive, we find that the PDC molecular weight would have to increase by a factor of 2.6, which is inconsistent with the DLS data. Therefore, the amount of aggregation consistent with the DLS data does not change the qualitative conclusion from the static light scattering data that PEG does not induce PDC attraction.

The light scattering experiments on PDCs, therefore, result in two apparently contradictory conclusions: one, that PEG does not induce PDC attraction as measured by virial coefficients and two, that PEG causes PDC aggregation as measured by DLS. We offer a speculative explanation: results from virial coefficient calculations on soluble proteins [26] demonstrate that negative second virial coefficient values are caused mainly by specific interactions between complementary surfaces at close distances. If a short ranged, but strong CLC-ec1 interaction led to irreversible aggregation, then this interaction would not contribute to the measured virial coefficient values, which reflect equilibrium properties. In light of this and our light scattering results, a hypothesis about the effect of PEG on CLC-ec1/OM PDCs can be made. PEG causes PDCs to aggregate irreversibly, possibly by destabilizing the detergent moieties on the PDCs thereby allowing specific short distance PDC interactions to occur. The fact that PEG destabilizes the OM micelles supports this hypothesis that the dominant effect of PEG on PDCs is through the detergent moieties. In this picture, some PDCs remain unaggregated in solution with net repulsive interactions, which is why the virial coefficients do not track the attraction associated with aggregation.

5. Conclusion

Protein/detergent complexes (PDCs) composed of CLC-ec1 and a non-ionic detergent, OM, were studied with static and dynamic light scattering experiments in conditions which yielded CLC-ec1 crystals. Both the apparent and effective second virial coefficients of these PDCs in their

crystallization conditions do not fall in the crystallization slot found for soluble proteins. No phase transition of the detergent micelles was associated with PDC crystallization. Calculation of the effective interactions between PDCs shows that the addition of PEG400 induces repulsion, rather than attraction between non-aggregated PDCs. However, PEG was found to destabilize detergent micelle formation and to induce CLC-ec1 PDC aggregation in crystal growth conditions.

Acknowledgments

The authors thank Professor C. Miller for providing all the materials for CLC-ec1 expression, isolation and purification, which were performed in his laboratory, and for advice on crystallization. We also wish to thank Dr. A. Accardi and C. Williams for their instructive assistance and helpful discussion. Research was funded by the NASA Office of Biological & Physical Research, Fundamental Microgravity Research in Physical Sciences (Fluid Physics) Grant # NAG3-2386.

References

[1] A. George, W.W. Wilson, Acta Cryst. D 50 (1994) 361.
[2] C. Hitscherich, et al., Protein Sci. 9 (2000) 1559.
[3] P.A. Marone, et al., J. Crystal Growth 191 (1998) 811.
[4] S. Tanaka, et al., Biophys. J. 84 (2003) 3299.
[5] J.P. Rosenbusch, J. Struct. Biol. 104 (1990) 134.
[6] C. Hitscherich Jr., et al., Acta Cryst. D 57 (2001) 1020.
[7] B.W. Berger, et al., Acta. Cryst. D 61 (2005) 724.
[8] T.L. Hill, An Introduction to Stastistical Thermodynamics, Addison-Wesley, Reading, MA, 1960.
[9] A.M. Kulkarni, et al., Phys. Rev. Lett. 83 (1999) 4554.
[10] J.G. Kirkwood, R.J. Goldberg, J. Chem. Phys. 18 (1950) 54.
[11] A. Vrij, Chem. Phys. Lett. 53 (1978) 144.
[12] R.S. King, H.W. Blanch, J.M. Prausnitz, AIChE J. 34 (1988) 1585.
[13] J. Bloustine, et al., Phys. Rev. Lett. 96 (2006) 087803.
[14] A. Vrij, Pure Appl. Chem. 48 (1976) 471.
[15] P. Tong, et al., J. Phys. France 51 (1990) 2813.
[16] H.D. Hek, A. Vrij, J. Colloid Interface Sci. 84 (1981) 409.
[17] M. Maduke, D.J. Pheasant, C. Miller, J. Gen. Physiol. 114 (1999) 713.
[18] J.A. Mindell, et al., Nature 409 (2001) 219.
[19] A. Accardi, et al., J. Gen. Physiol. 123 (2004) 109.
[20] A. Accardi, C. Miller, Nature 427 (2004) 803.
[21] R. Dutzler, et al., Nature 415 (2002) 287.
[22] W. Kaye, A.J. Havlik, Appl. Opt. 12 (1973) 541.
[23] D.E. Koppel, J. Chem. Phys. 57 (1972) 4814.
[24] B.J. Bern, A. Pecora, Dynamic Light Scattering, Wiley, New York, NY, 1976.
[25] B.J. Boyd, et al., Langmuir 16 (2000) 7359.
[26] B.L. Neal, et al., J. Crystal Growth 196 (1999) 37.